Journal Pre-proof

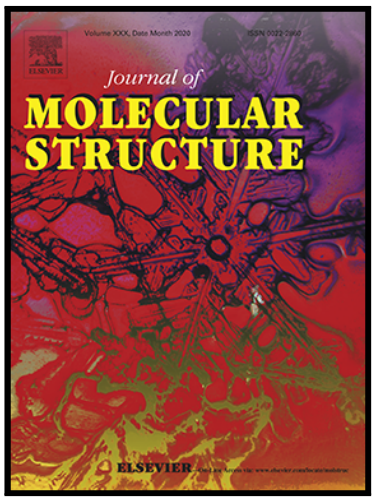

Decavanadate Salts of Piperidine and Triethanolamine: A Combined Experimental and Theoretical Study

Rim Zarroug , Anissa Haj Abdallah , Philippe Guionneau , Albert Masip-Sánchez , Xavier López , Brahim Ayed

PII: S0022-2860(21)00810-3
DOI: https://doi.org/10.1016/j.molstruc.2021.130677
Reference: MOLSTR 130677

To appear in: *Journal of Molecular Structure*

Received date: 1 December 2020
Revised date: 6 May 2021
Accepted date: 7 May 2021

Please cite this article as: Rim Zarroug , Anissa Haj Abdallah , Philippe Guionneau , Albert Masip-Sánchez , Xavier López , Brahim Ayed , Decavanadate Salts of Piperidine and Triethanolamine: A Combined Experimental and Theoretical Study, *Journal of Molecular Structure* (2021), doi: https://doi.org/10.1016/j.molstruc.2021.130677

This is a PDF file of an article that has undergone enhancements after acceptance, such as the addition of a cover page and metadata, and formatting for readability, but it is not yet the definitive version of record. This version will undergo additional copyediting, typesetting and review before it is published in its final form, but we are providing this version to give early visibility of the article. Please note that, during the production process, errors may be discovered which could affect the content, and all legal disclaimers that apply to the journal pertain.

© 2021 Published by Elsevier B.V.

Highlights

- Tow hybrid decavanadate were prepared by aqueous solution
- The structures were established with of single crystal X-ray crystallography.
- Using Several spectral analyses like HSA/ MEP/DFT for characterisation

Journal Pre-proof

Journal Pre-proof

Decavanadate Salts of Piperidine and Triethanolamine: A Combined Experimental and Theoretical Study

Rim ZARROUG [a,b] , Anissa HAJ ABDALLAH [c], Philippe GUIONNEAU[d],Albert MASIP-SÁNCHEZ[e], Xavier LÓPEZ[e] and Brahim AYED [a,c]

[a]University of Monastir, Laboratory of Physico-chemistry of Materials LR01ES19, Faculty of Sciences,Tunisia

[b] Department of chemistry,Faculty of Sciences, University of Gabes, Tunisia

[c]Research Unit of Analysis and Process Applied to the Environment (UR17ES32)-ISSAT Mahdia, University of Monastir, Tunisia

[d]CNRS, Univ. Bordeaux, Bordeaux INP, ICMCB, UMR 5026, 87 av. Dr A. Schweitzer, F-33600 Pessac (France)

[e] Universitat RoviraiVirgili, Departament de QuímicaFísicaiInorgànica, Marcel·lí Domingo 1, 43007 Tarragona, Spain

Abstract

Two novel decavanadate salts with organic cations, $(C_5H_{12}N)_4[H_2V_{10}O_{28}]\cdot 3.25H_2O$ (**I**) and $(C_6H_{12}N(OH)_3)_2[H_4V_{10}O_{28}]\cdot 10H_2O$ (**II**), have been synthesized in aqueous solution and characterized by IR, UV-Vis spectroscopies, EDX-SEM and single crystal X-Ray diffraction completed by DFT calculations. The asymmetric unit of $(C_5H_{12}N)_4[H_2V_{10}O_{28}]\cdot 3.25H_2O$ is composed of one decavanadate $[H_2V_{10}O_{28}]^{4-}$, four piperidinium cations and water molecules. The structures of **(II)** is based on one decavanadate cluster, two triethanolaminum cations $(TEAH)^+$ and ten water molecules. The cohesion of the crystal packing in both compounds is provided by a complex network of N-H ⋯ O, O_w-H ⋯O and O-H ⋯O hydrogen bonds involving water molecules and organic molecules as well as vander Waals interactions for the

connection between the organic molecules. The IR spectra confirmed the presence of organic cations, decavanadate $(V_{10}O_{28})^{6-}$ groups and water molecules. The UV-Vis diffuse reflectance spectrum shows that these compounds exhibit semiconducting behavior with an optical band gap of 2.22 eV and 2.13 eV respectively for compound (**I**) and (**II**).Furthermore the Hirshfeld surface analysis shed more light on the intermolecular interactions occurring in the two crystals and the structure-properties relationships.

Keywords: Inorganic-organic hybrids, Decavanadate, X-ray Diffraction, IR Spectroscopies, UV-visible Spectroscopies, Hirschfeld surfaces, DFT calculations.

1- Introduction

Polyoxometalates (POMs) are a class of hybrid organic-inorganic metal oxide materials formed from early-transition metals in their highest oxidation states (V, Nb, Mo, W…). The physico-chemical properties of POMs allowed them to be envisaged in various applicative devices in different fields such as catalysis, energy storage, medicine, magnetism and electrochromic applications… **[1-3]**.

Polyoxovanadates (POVs) are a subfamily of POM compounds characterized by atomic architectures different than those found for classical POMs. Among POVs, the decavanadate anion is a well-known isopolyoxovanadate stable in acidic medium and recognized as a biologically active chemical system. This entity of general formula $[H_nV_{10}O_{28}]$ can be found in different protonation states such as $[H_nV_{10}O_{28}]^{(6-n)-}$ with n= 1–4 depending first on the chemical acidity range of then on the medium and the nature of the counter ion. **[4]**

A variety of POV species are structurally characterized by single crystal X-ray diffraction. As examples we can note the following anions: $[V_2O_7]^{4-}$ **[5]**, $[V_3O_9]^{3-}$**[6]**, $[V_4O_{12}]^{4-}$**[7]**, $[V_5O_{14}]^{3-}$ **[8]**, $[V_{10}O_{28}]^{6-}$ **[9]**, $[V_{12}O_{32}]^{4-}$**[10]**, $[V_{13}O_{34}]^{3-}$ **[11]**, $[V_{15}O_{42}]\ ]^{9-}$**[12]y**$[V_{16}O_{42}]^{4-}$**[13]**.

Journal Pre-proof

This paper reports a detailed study of the synthesis, single-crystal X-ray diffraction and IR spectroscopy characterization of two new decavanadates, $(C_5H_{12}N)_4[H_2V_{10}O_{28}]\cdot 3.25H_2O$ **(I)** and $(C_6H_{12}N(OH)_3)_2[H_4V_{10}O_{28}]\cdot 10H_2O$ **(II).**Furthermore, theoretical calculations using DFT applied to POVs supplemented by the calculation of the topologies of interatomic contacts from the experimental structural data (Hirshfeld surfaces)can provide useful information about the characteristics of interactions and energy, and also additional insight on the electronic structure in terms of molecular orbitals and of derived properties such as the molecular electrostatic potential and the electron density distribution, to name a few.**[14]**We therefore propose here to apply such approach to the two new synthesized POVs by combining spectroscopies (IR, UV, EDX), X-ray diffraction (single-crystal and powder) as well as DFT.

2- Experimental:

2.1. Materials and measurements:

For the titled compounds, all reagents were purchased commercially and used without any further purification. The infrared spectra of $(C_5H_{12}N)_4[H_2V_{10}O_{28}]\cdot 3.25H_2O$ (**I**) and $(C_6H_{12}N(OH)_3)_2[H_4V_{10}O_{28}]\cdot 10H_2O$ (**II**) were recorded at room temperature with a Perkin Elmer Spectrum. Tow ATR FTIR between 4000 and 400 cm^{-1}.UV–visible diffuse reflectance spectra are collected on an UV–visible two-channel spectrometer Cary 5 from Carian Techtron Pty., Darmstadt, using $BaSO_4$ as white standard. Optical electronic properties are evaluated applying the Kubelka-Munk method **[15]**.Energy dispersive X-ray analyses (EDX) are done on a Philips Environmental Scanning Electron Microscope ESEM XL30 with an EDX detector. Powder X-ray Diffraction (PXRD)pattern and CHN analyses support the compositions determined from the Single-Crystal X-ray Diffraction (SCXRD) crystal structure determination.

Journal Pre-proof

*2.2. Chemical preparation and crystallization of compounds **I** and **II***

The decavanadate complexes of Piperidinium, $(C_5H_{12}N)_4[H_2V_{10}O_{28}]\cdot 3.25H_2O$ (**I**) and Triethanolaminium, $(C_6H_{12}N(OH)_3)_2[H_4V_{10}O_{28}]\cdot 10H_2O$ (**II**), have been prepared as described below and isolated from aqueous solutions.

*2.2.1. Synthesis of $(C_5H_{12}N)_4[H_2V_{10}O_{28}].3.25H_2O$ (**I**)*

Compound (**I**) was synthesized by dissolving ammonium metavanadate (0.06g, 0.5 mmol) and piperidine (0.03 mL, 3.03 mmol) into H_2O (20mL) in a round-bottom flask. The solution was adjusted to a pH of 3.8 by adding acetic acid dropwisely and then heated at 65^{o}C for 48h. After the reaction the mixture was filtered and the yellow filtration evaporated slowly in the open air at room temperature. A few weeks' later orange small crystals suitable for X-ray diffraction analysis were separated from the liquid with 40% yield. Qualitative analysis (**Fig.1a**) of these crystals by electron microscope probe revealed the presence of the V, O, N and C atoms.*Elem. Anal.Found*: C, 16.837; H4.466; N,5.426 (%). Calcd: C, 17; H, 4; N, 4 (%).

*2.2.2. Synthesis of $(C_6H_{12}N(OH)_3)_2[H_4V_{10}O_{28}].10H_2O$ (**II**)*

Product (**II**) has been obtained from a solution of (0.03mL;2.27mmol) of Triethanolamine in 10 mL of water which was added to a suspension of NH_4VO_3 (0.06 g, 0.05 mmol) in 20 mL of water. After stirring and heating under reflux for 3h, the suspension was filtered under vacuum. Yellow crystals formed as soon as the solution cooled down to room temperature and were dried in air.

The qualitative analysis by EDX spectrum and SEM micrographs (**Fig.S1**) of one of the yellow stick-like crystals obtained revealed the presence of only V, C, N and O elements. Elem. Anal. Found: C10.357; N, 5.741; H, 4.195 (%). Calc: C, 10; N, 2; H, 3.5 (%).

Journal Pre-proof

2.2.3 X-Ray Powder Diffraction Pattern of Compound (I) and (II)

The homogeneity of the powders of phase (**I**) and (**II**) were checked by comparing, using the Origin software **[16]**, the experimental diffractogram (λ_{Mo} (Kα1) = 0.71073Å) with the calculated diffractogram from single-crystal X-ray diffraction data (see below), obtained using the VESTA program **[17]**. The superposition of the two diffractograms (**Fig.S2a** and **S2b**) and their very good overlapping confirms that the two synthesized powders does correspond to compounds (**I**) and (**II**) respectively without any significant presence of other phases.

2.3. Electronic structure calculations

The decavanadate anion was also analyzed with quantum mechanical calculations. Density Functional Theory calculations (DFT) were carried out with the ADF2017 suite of programs**18]**. For the geometry optimization, we applied the BP86 GGA-like functional**[19]** with a triple-z+ polarization basis set for all atoms, whereas a single point run with the B3LYP hybrid-type functional**[20]**was carried out to obtain the final electronic structure. Both runs accounted for the effects of an aqueous solution on the target molecule by means of the Conductor-like Screening Model (COSMO)**[21]** to mimic the experimental conditions.To save computational time, the internal electrons were treated with the *frozen core* approximation (1s for oxygen; 1s-2p for vanadium).Scalar relativistic effects via the Zeroth-Order Regular Approximation (ZORA)**[22]** were considered.

2.4. Single-Crystal X-ray Diffraction

Both compounds are stable under ambient conditions and two single crystals were carefully selected and glued at the end of a glass capillary. The intensities of the diffraction data were measured using a Nonius Kappa CCD diffractometer with monochromated graphite Mo K□ radiation (» =0.71073 Å) at 293 K. A single crystal of **(I)** was carefully selected and glued on the end of a glass capillary. The X-ray diffraction data were collected in the range of 2.9<

Journal Pre-proof

θ<27.9. A total of 32950 reflections(6347unique) were measured (-37 < h < 37, -25 < k < 23, -22< l < 24) and multi-scan absorption correction was applied. The structure was solved by direct methods using SIR-97 **[23]** and refined by full-matrix least-squares on F^2using the SHELXL-97 software **[24]**. All non-hydrogen atoms were refined anisotropically. The hydrogen atoms attached to nitrogen and carbon atoms were fixed in ideal positions and treated as riding on their parent atoms; other hydrogen atoms were partially located. For compound (**II**) the numbers of collected and independent reflections were respectively, 27787 and 5221. Unit cell dimensions were obtained by least-square refinement of the angular settings in the 3.3 < θ< 27.9. The structure was successfully developed in the centrosymmetric space group Pbca, solved by Patterson method using SHELXS97 and refined with anisotropic temperature factors for no hydrogen atoms, by full matrix leastsquares based on F^2 using SHELXL-97. The final full-matrix least-squares refinement on F^2 converged with R = 0.034 and wR(F2) = 0.102 for 4267 unique observed reflexions [I > 2s(I)]. Crystal parameters and details of the data collection and refinement for structure (I) and (II) are listed in **Table 1**. Molecular graphics are made with Diamond 2.1.

3. Results and discussion

3.1. Crystal-structure description

The identity of (**I**) and (**II**) was elucidated by single crystal X-ray diffraction analysis. Investigated compounds crystallize in the monoclinic *C*2/c(**I**) and Orthorhombic Pbca (**II**) space groups respectively with one decavanadate $[H_nV_{10}O_{28}]^{(6-n)-}$ anion, organic cations and several water molecules in the asymmetric unit of the crystal lattice. A projection of the structure of (**I**) and (**II**) showing the displacement ellipsoids are presented in (**Fig.1a** and**Fig.1b)**respectively. The number of above-mentioned solvent molecules in the independent part of unit cell is respectively 3.25 and 5 in case of (**I)** and (**II)**. The crystal data and structure refinement details for all compounds are summarized in Table 1.

Journal Pre-proof

The polyanion $[V_{10}O_{28}]^{6-}$ in(**I)** is a POMs structure containing ten fused $[VO_6]$ octahedra via edge sharing. For compound (**II)**, the centrosymmetric polyanions $[V_{10}O_{28}]^{6-}$ consists of five independent $[VO_6]$ octahedra sharing edges and has approximate D_{2h} symmetry.

The V–V distances are in the range 3.0570(2)–3.1145(1) Å for (**I**) and 3.0629(8)–3.0945(9) Å for (**II**). In the structure of the decavanadate clusters, four different categories of oxygen atoms are found (O_t, μ_2, μ_3, and μ_4). The bond lengths between V - (O_t) are in the ranges of 1.5933(29)–1.6085(27)Å for (**I**) and 1.6028(19)–1.6085(16) Å for (**II**).The double joined oxygen atoms exhibit a bond length 1.6797(26)–2.0881(27)Å and 1.6737(16)–2.0697(19) Å(μ_2).1.8971(27)–2.0273(25) Å and 1.9211(16)–2.0223(18) Å are the bond length between tripleμ_3 joined oxygen and vanadium atoms. Bond lengths corresponding to distances between fourth joined oxygen atoms and vanadium 2.101(25)–2.3017(27) Å and 2.0953(17)–2.3263(17) Å (μ_4) for (**I**) and (**II**). Those values are respectively, comparable with those found in other decavanadate polyanions **[25-28]**.Selected bond lengths of (I) and (II) are listed in **Tables 2**and**3.**

Using the labelling in the **Fig.S3**, three types of V positions can be distinguished for $V_{10}O_{28}$: apical ($V_{3,6,8,9}$), plane-internal ($V_{1,5}$) and plane-external ($V_{2,4,7,10}$). Four main types of oxygens can be distinguished: terminal (8 in total), μ_2-bridging in-plane or out-of-plane(14), μ_3-bridging (4) and internal μ_4 (2).

Table S1 shows that, in general, computed and measured distances compare quite well and, thus, the DFT structure represents properly the characteristics of the POM crystal obtained. As the imposed symmetry of the calculated structure is C_i, it captured the distorted nature of the structure, that is, an irregular distribution of the distances. From the table, some features stand out: the V(plane)-O(μ_2) in-plane distances cover a wider range of values than the V(plane)-O(μ_2) out-of-plane ones; the V(internal)-O(μ_4) bonds are clearly shorter than the V(other)-O(μ_4) ones; the V-O(terminal) distances are, overall, the shortest ones in average,

Journal Pre-proof

attributed to their pseudo double bond nature. The biggest deviations observed between X-ray and DFT distances are found in some short distances, such as the V-O(terminal) ones, which are rather long in the DFT version with respect to the X-ray ones. Such an expected effect is due to the approximate treatment of the POM environment. While the X-ray geometry corresponds to a crystal packing and, thus, a compressed structure, the DFT one is obtained by applying the approximate solvent model COSMO, which cannot account for the compression exerted on the POM in the real crystal. Even though, this deviations are not changing the main features of the electronic structure of the system, as multiple publications on this field has shown before **[21]**.

The O–V–O angle deviations, from 90^{o} for cis-standing oxygen atoms and from 180^{o} for trans-standing oxygen atoms, also reflect the extent of distortion within the VO_6 octahedra. Indeed, the angle ranges cover 72.65(1)–105.03(13)^{o} (**I)** and 74.17(6)– 104.63(9)^{o}**(II)** for cis-standing oxygen atoms and 154.06(12)–174.67(13)^{o} (**I)** and 154.26(7)–174.51(9)^{o} (**II**) for trans-standing oxygen atoms, consistent with $[V_{10}O_{28}]^{6-}$ clusters observed in other compounds **[29]** and **[30]**. The full list of angles can be found in the supporting information (**Table S2**and**Table S3**).

It can be seen that the V–O bond lengths and the values of the O–V–O valence angles intervals in (**I)**-(**II)**are slightly different and this difference may be due to the influence of the different number of water molecules and the various shape of the organic cations, i.e. it reflects the influence of the surroundings entities within the crystal packings.

The angles and bonds within the VO_6 polyhedrons show that the octahedrons are distorted. The distortion indices were calculated using the Baur method **[31]**.The resulting parameters are ranged from 0.077 to 0.1 for ID (V–O) and 0.132 to 0.234 for ID(O–V–O) for compound (**I)** and from 0.077 to 0.088 for ID(V–O) and 0.221 to 0.225 for ID(O–V–O) for compound (**II)**.

Journal Pre-proof

BVS calculations using the Brown and Altermatt method **[32]** revealed that all the vanadium atoms have valence sums ranging from 4.975 to 5.010 (**I**) and from 4.806 to 5.009 (**II**) with an average value of 4.993 for (**I**) and 4.989 for (**II**), close to the ideal value of 5 for V^{V}. The bond valences of oxygen atoms in the two compounds are in the range of 1.689 to 1.764 valence units for terminal oxygen atoms and 1.681–2.002 valence units for bridging oxygen atoms, except 1.423 for O(9) and 1.11 for O(11) in compound (**I**) also in compound (**II**) 1.496 for (O8) and 1.495 for O(3), indicating that in each compound the cluster is a diprotonated core and the protonation occurs at O(9) and O(11) for (**I**) and at O(8) and O(3) for (**II**).

*3.1.1. Compound $(C_5H_{12}N)_4[H_2V_{10}O_{28}].3.25H_2O$(**I**)*

Single crystal X-ray diffraction analysis reveals that compound (**I**) is based on a relative proportion of four cations, one decavanadate and 3.25 water molecules crystallization. A projection of the crystal structure is shown in **Fig.2**. The two $[H_2V_{10}O_{28}]^{4-}$ are bound by short hydrogen bonds to the four cations $[C_5H_{12}N]^{+}$and are polymerized to form pseudo-1D chain. The chain is spread along the crystallographic **b** axis and **c** axis. The adjacent inorganic-organic chains are also joined to produce a 3D supramolecular architecture through a complex network of N-H ⋯ O, O_w-H ⋯O and O-H ⋯O hydrogen bonds and van der Waals interactions between cations pipiredium, water molecules and polyoxoanions.

The piperidine ligand is in the chair form, with a CNC angle of 113.97(0)°; the CCC angle opposite the nitrogen atom is 110.35(2)°.The two NCC angles average to 109.85(5)°; the remaining two CCC angles average to 111.82(1)°.The excellent agreement between structurally independent, chemically analogous bond lengths is maintained in the piperidine ligand with average values of $(N\text{-}C)_{av}$= 1.489(5) Å and $(C\text{-}C)_{av}$= 1.516 (5) Å.

The inter-atomic distances and angles describing organic cations are similar to the distances and angles of the intramolecular bonds usually reported for these species **[32]**.

Journal Pre-proof

The hydrogen bonding extended in the crystalline structure of (**I**) is listed in **Tables 4**, the hydrogen bond N-H⋯ O between the complex cation $[C_5H_{12}N]^+$ and the oxygen atoms of the decavanadate units with interatomic distances N⋯O ranging from 2.76(5) to3.13 (6) Å and angles N-H⋯O between 115.77° and 175.47°. It should be noted that compound (**I**) has hydrogen bonds O-H ⋯ O between the O-H groups of the water molecule and the oxygen atoms of the decavanadate units have inter-atomic distances O⋯O from 2.69 (1) to 3.06(6) Å. These hydrogen bonds hold the components together in a three-dimensional network and make the crystalline structure of the compound more stable.

*3.1.2. Compound ($C_6H_{13}N(OH)_3)_2[H_4V_{10}O_{28}].10H_2O$(**II**)*

The structures of (**II**) are constructed by decavanadate clusters, two triethanolaminumcations $(TEAH)^+$ and water molecules.

As seen in **Fig.2** the structure of (**II**) can be described as a 3D supramolecular architecture formed by decavanadate clusters, triethanolaminium cation and water molecules which are linked through a complex network of hydrogen bonding and van der Waals interactions.

The variety of hydrogen bonds O–H⋯O, O_W–H ⋯O_W and O_W–H⋯O enhance the stability of the crystalline building. The geometric characteristics of the hydrogen bonds are described in **Table 5**. The majority of the interactions are between the terminal oxygen atoms of the clusters and the hydrogen atoms of the hydroxide group of the organic molecule.

The interatomic distances and angles describing the organic cation are similar to intramolecular bond distances and angles usually reported for such species. The characteristic C–O distances of $TEAH^+$ range from 1.404(1) Å to 1.424(1) Å, which is the normal C–O bond distance in organic molecules. **[33-35]**

Journal Pre-proof

*3.2. IR spectroscopy Study of Compound (**I**) and (**II**)*

The FT-IR spectra of the two compounds in KBr pressed pellets is presented in (**Fig.S4**). The characteristic peaks in the range 945-502 cm^{-1} for (I) and 929-502 cm^{-1} for (II), show the polyoxoanion keep decavanadate structure **[36].**

The spectra of (I) and (II) display the terminal $V=O_t$ stretching bond within the range 950-900 cm^{-1} and those at about 810 and 833 cm^{-1} to the asymmetric stretching vibration of $V–O_{b/c}–V$. The bands between 588 and 502 cm^{-1} can be assigned to the (V–O–V) remaining stretchings. The lattice water absorption bands centeredat 3554 cm^{-1} and 3402 cm^{-1} are more intense in (**II)**than in (**I)** which is in agreement with its major water content.

The peaks from 1034 to 1458 cm^{-1} could be regarded as the characteristics of the organic molecules: The bands from 1170 to 1458 cm^{-1} can be attributed to the C–H in-plane bending vibrations. The pipiredinium ring stretching give rise to two bands at 3407 and 1592 cm^{-1} **[37]** for compound (**I)** and the medium bands at 1088 and 1034cm^{-1} were attributed to the v(C-O) and v(C-N) in triethanolamine **[39]** for compound (**II).** These results are fully coherent with the SCXRD ones.

*3.3. Optical properties UV-vis region of Compound (**I**) and (**II**)*

To evaluate electronic transitions from UV–vis data, the Kubelka-Munk**[15]** relationship has been applied. The measurement of the reflectance spectrum shows that this compound is a semiconductor material. The absorption peaks observed at 460 nm and 420 nm for the two compounds (**I**) and (**II**) respectively(**Fig.S5**)can be assigned to the ligand-metal charge transfer (LMCT) from terminal oxygen to the vanadium center ($O_t \rightarrow V$) and responsible for the typical yellow or orange color of vanadium solutions for the two compounds **[40]**.

The band gap values of 2.22 eV and 2.13 eV respectively for compound (**I**) and (**II**), were determined from the plot of the curve $(ah)^2$ versus h, (**Fig.3**) by extrapolating the linear

Journal Pre-proof

portion near the onset of the absorption edge at the energy axis. The optical band gap definitively shows that the two compounds exhibit semiconducting behavior.

3.4. Hirshfeld Surface Analysis (HSA)

Intermolecular interactions and the distribution of electron densities in the crystal structure were analysed using the CIF file within the Crystal Explorer package **[41]** using the Hirschfield surface (HS) mapped with the d_{norm} function **[42]**, which contributes to the qualitative evaluation of intramolecular interactions in the crystal lattice. Global interactions and their contribution to SH construction is then quantified using 2D fingerprints **[43].**

The normalized contact distance (d_{norm}) based on two types of distances, of de and di representing the external / internal distance between the point and the nearest core at the surface **(Fig.4**and**Fig.6)**.

The 2D fingerprint plots **(Fig.5)** for compound**(I)** provide us with information about these intermolecular interactions. It appears from the plots that the O ⋯ H / H ⋯ O bond (50.9%) are the major factor in the crystal packing whereas H ⋯ H (37.9%), O ⋯ O (7.5%) and O ⋯ N / N ⋯ O (3.7%) contacts have also their significant contribution to the total area of the surface. The remaining contacts are negligible. For compound (**II)**, the 2D fingerprint plots **(Fig.7)** provide us with information about these intermolecular interactions. It appears also from the plots that the O⋯ H / H ⋯ O bond (61.7%) are the major factor in crystal settlement, whereas H ⋯ H (21.6%), O ⋯ O (12%), O ⋯ V / V⋯ O (4.6%) and V ⋯ H / H ⋯ V bond (0.2%) contacts have their significant contribution to the total area of the surface. The remaining contacts are negligible.

3.5. Frontier molecular orbital analysis (FMO)

From DFT calculations we obtained the electronic structure of the $[V_{10}O_{28}]^{4-}$system in aqueous solution conditions. The most relevant molecular orbitals for the majority of physico-chemical properties, namely the Highest Occupied MO and the Lowest Unoccupied

Journal Pre-proof

MO (HOMO and LUMO, respectively) are illustrated in(**Fig.8)**. As usual in POM compounds, the HOMO and other occupied orbitals close in energy present contributions of the bridging oxygen atoms principally**[44].** On the other hand, the LUMO and other virtual orbitals are made of combinations of metal d valence orbitals. The HOMO-LUMO gap establishes the energy range at which electromagnetic radiation can be absorbed for (**I)** and **(II)**, and to identify its chemical reactivity and kinetic stability. The B3LYP results give HOMO and LUMO energiesof–7.00 and–2.97 eV, respectively, which denote notable chemical stability in aqueous medium. In relation to this, a large HOMO-LUMO energy gap of ΔE = 4.03 eV was computed. The results allow us to consider compound (**I)** and (**II)** to have electronic characteristics of a semiconductor, which confirm the experimental investigation.

3.6. Molecular electrostatic potential

To visualize the relative polarity and active sites of molecules we can use molecular electrostatic potential (MEP) maps. The electrostatic potential is a scalar function that, in quantum mechanical molecular calculations, can be derived from the electron density.MEP representations provide a simple pictorial method to grasp some fundamental surface molecular properties such as molecular nucleo- and electrophilicity, which has revealed very useful in the theoretical study of POMs**[45]**.The 3D mapped surface of the MEP is shown in (**Fig.9)** According to the MEP map, the different values at the surface are represented by a color scale ranging from red (more negative potential) to blue (less negative or positive potential). As expected, the most negative potential regions are mainly localized at bridging oxygens of the decavanadate anion**[46]**, the most nucleophilic sites. In consequence, these regions are susceptible for an electrophilic attack by a cation or the positive pole of another molecule. The light green, yellow and orange regions (i.e., terminal oxygens) are somewhat less nucleophilic than bridging ones, in relation with a potential halfway between the two

Journal Pre-proof

extremes in red and blue colors. It reinforces the idea that protonation of the decavanadate anion takes place preferentially **[9]**, and in an itinerant way, in the bridging oxygen located at both 'hemispheres' of the molecule.

Conclusion

In summary conventional aqueous solutions method synthesis has permitted the self-assembly of two new inorganic-organic hybrid supramolecular decavanadate clusters. The compounds are characterized by X-ray diffraction, UV and IR spectra completed by EDX. Compound (I) is composed of one decavanadate $[H_2V_{10}O_{28}]^{4-}$, four piperidinium cations and water molecules. The structures of **(II)** are mainly constructed by decavanadate clusters, two triethanolaminum cations $(TEAH)^{+}$ and ten water molecules. The cohesion is provided by a complex network of N-H ⋯ O, O_w-H ⋯O and O-H ⋯O hydrogen bonds involving water molecules and organic molecules, and van der Waals bonds for the connection between the organic molecules. Spectroscopic investigation is coherent in all points with the Single-crystal X-ray structural analyses. The optical band gap shows that the two compound exhibits semiconducting behaviour. Hirshfeld surface analyses, especially d_{norm} surface and fingerprint plots were used for decoding the intermolecular interactions topology in each crystal packing.

Supplementary material

CCDC 2044661 and 1902735, contain the supplementary crystallographic data for this paper. These data can be obtained free of charge via http://www.ccdc.cam.ac.uk/data_reque st/cif, by e-mailing data_request@ccdc.cam.ac.uk or by contacting The Cambridge Crystallographic Data Centre, 12 Union Road, Cambridge CB2 1EZ, UK. Fax: +44 1223 336033.

Journal Pre-proof

References

[[**1]** M.T. Pope, Heteropoly and IsopolyOxometalates (1983).

[2] M.T. Pope, A. Muller, Polyoxometalate Chemistry From Topology via Self Assembly to Applications, (1994).

[3] H. Ratajczak, A.J. Barnes, A. Bielański, H.D. Lutz, A. Müller, M.T. Pope Vibrational Spectroscopy of Heteropoly Acids, (2001).

[4] E. Sánchez-Lara, A. Pérez-Benítez , S. Treviño, A. Mendoza , F. J. Meléndez,E. Sánchez-Mora, S. Bernèsand, E. González-Vergara, Synthesis and 3D Network Architecture of 1-and 16-Hydrated Salts of 4-Dimethylaminopyridinium Decavanadate, $(DMAPH)_6[V_{10}O_{28}]nH_2O$, Crystals 6 (2016) 65-77.

[5] (**a**) W. Bensch, P. Hug, A. Reller and H.R. Oswald, The crystal structure of di(propane(1,3)diammonium)divanadate, Mater. Res. Bull. 24 (1989) 403-415.

(**b**) S. Aschwanden, H.W. Schmalle, A. Reller and H.R. Oswald, Preparation, crystal structure and thermal behaviour of cobalt-ethylenediamine-vanadate, Mat. Res. Bull. 28 (1993) 575-590.

[6] E.E. Hamilton, P.E. Fanwick and J.J. Wilker, The elusive vanadate $(V_3O_9)^{3-}$: Isolation, crystal structure, and nonaqueous solution behavior, J. Am. Chem. Soc. 124 (2002) 78-82.

- **[7] (a)** W.G. Klemperer, W. Shum, charge distribution in large polyoxoanions: Determination of protonation sites in vanadate $V_{10}O_{28}^{6-}$ by oxygen 17 nuclear magnetic resonance,angew. Chem. Int. Ed. Engl., 15 (197) 3544-3545.

(**b**) G.Y. Yang, D.W. Gao, Y. Chen, J.Q. Xu, Q.X. Zeng, H.R. Sun, Z.-W. Pei, Q. Su, Y. Xing, Y.H. Ling, H.Q. Jia, $[Ni(C_{10}H_8N_2)_3]_2[V_4O_{12}].11H_2O$, Acta Cryst. C: Cryst. Struct. C 54 (1998) 616-618.

[8] V.W. Day, W.G. Klemperer, O.M. Yaghi, A new structure type in polyoxoanion chemistry: Synthesis ant structure of the $V_5O_{14}^{3-}$ anion , J. Am. Chem. Soc., 111 (1989) 4518-

Journal Pre-proof

4519.

[9] V. W. Day, W. G. Klemperer, D. J. Maltbie, where are the protons in $H_3V_{10}O_{28}^{3-}$, J. Am. Chem. Soc., (1987) 2991-3002.

[10] (**a**) V. W. Day, W. G. Klemperer, O. M. Yaghi, Synthesis and Characterization of a Soluble Oxide Inclusion Complex, [CH_3CN.cntnd. ($V_{12}0_{32}^{4-}$)]J. Am. Chem. Soc. 111 (1989) 5959-5961.(**b**) W.G. Klemperer, T.A. Marquart, O.M. Yaghi, Shape-selective binding of nitriles to the inorganic cavitand $V_{12}O_{32}^{4-}$, Mater. Chem. Phys. 29 (1991) 97-104.

(**c**) N. Kawanami, T. Ozeki, A. Yagasaki, NO- Anion Trapped in a Molecular Oxide Bowl, J. Am. Chem. Soc., 122 (2000) 1239–1240.

[11] D. Hou, K.D. Hagen, C.L. Hill, Tridecavanadate, $[V_{13}O_{34}]^{3-}$, a new high potential isopolyvanadate, J. Am. Chem. Soc. 114 (1992) 5864-5866.

[12] D. Hou, K.S. Hagen, C.L. Hill, Pentadecavanadate , $V_{15}O_{42}^{9-}$,a new highly condensed fully oxidized isopolyvanadate with kinetic stability in water, J. Chem. Soc., Chem. Commun. 4 (1993) 426-482.

[13] J. Marrot, K. Barthelet, C. Simonnet, D. Riou, A Bowl-Type Dodecavanadate as a Halide Receptor, C. R.Chim. 8 (2005) 971-976.

[14](a) N. Vilà, P.A. Aparicio, F. Sécheresse, J.M. Poblet, X. López, I.M. Mbomekallé, Electrochemical Behavior of α_1/α_2-$[Fe(H_2O)P_2W_{17}O_{61}]^{7-}$ Isomers in Solution: Experimental and DFT Studies,Inorg. Chem. 51 (2012) 6129–6138.

(b) M. Vonci, F.A. Bagherjeri, P.D.Hall, R.W. Gable, Y. Liu, J. Zhang, M. Field, M. Taylor, J. Du Plessis, G. Bryant, M. Riley, L. Sorace, P.A. Aparicio, X.López, J.M. Poblet, C. Ritchie, C. Boskovic, Modular Molecules: Site-Selective Metal Substitution, Photoreduction, and Chirality in Polyoxometalate Hybrids ,Chem. Eur. J. 20 (2014) 14102–14111.

(c) A. Notario-Estévez, P. Kozłowski, O. Linnenberg, C. de Graaf, X. López, K. Yu Monakhov, Decoding the role of encapsulated ions in the electronic and magnetic properties

Journal Pre-proof

of mixed-valence polyoxovanadate capsules $\{XV_{22}O_{54}\}$ ($X = ClO_4^-$, SCN^-, $VO_2F_2^-$): a combined theoretical approach., Phys. Chem. Chem. Phys. 20 (2018) 17847–17858**.**

(d) X. López, J.J. Carbó, C. Bo, J.M. Poblet, Structure, properties and reactivity of polyoxometalates: theoretical perspective ,Chem. Soc. Rev. 41 (2012) 7537–7571.

[15] T.M. Anderson, T.M. Alam, M.A. Rodriguez, J.N. Bixler, W. Xu, J.B. Pariseand, M. Nyman, Cupric Siliconiobate. Synthesis and Solid-State Studies of a Pseudosandwich-Type Heteropolyanion , Inorg. Chem. 47 (2008) 7834–7839.

[**16**] Microcal Origin Version 8.0 (1991-2009). Microcal Software Inc. One, Northampton.

[**17**] K. Momma, F. Izumi, Preparation, crystal structure and spectroscopy characterization of vanadium (V) Complex,2-amino-pivolinium,2-methylimidazolium decavanadate hydrate ,J. Appl. Cryst. 44 (2011) 1272–1276.

[18] G. teVelde, F.M. Bickelhaupt, E.J. Baerends, C. Fonseca Guerra, S. J. A. van Gisbergen, J.G. Snijders, T. Ziegler, Chemistry with ADF, J. Comput. Chem.2 2 (2001) 931–967.

[19](a) A. D. Becke, Density-fnnctional exchange-energy approximation with correct asymptotic behaviour, Phys. Rev. A 38 (1988) 3098–3100.

(b) J.P. Perdew, Density functional approximation for the correlation energy of the inhomogeneous electron gas, Phys. Rev. B, 33 (1986) 8822–8824.

[20] P. J. Stephens, F. J. Devlin, C. F. Chabalowski, M. J. Frisch, Ab Initio Calculation of Vibrational Absorption and Circular Dichroism Spectra Using Density Functional Force Fields, J. Phys. Chem. 98 (1994) 11623–11627.

[21]C.C. Pye, T. Ziegler, An implementation of the conductor-like screening model of solvation within the Amsterdam density functional package, Theor. Chem. Acc. 101 (1999), 396-408.

[22] E. van Lenthe, E.J. Baerendsand J.G. Snijders, Relativistic regular two-component Hamiltonians , J. Chem. Phys., 99 (1993) 4597-5600.

Journal Pre-proof

[**23**] L.J. Farrugia, WinGX suite for small molecule single-crystal crystallography, J. Appl. Crystallogr. 32 (1999) 837-838.

[24]G.M. Sheldrick, SHELXS97 and SHELXL97. Program for Crystal Structure Solution and Refinement, University of Gottingen, Germany, (1997).

[25] A.G. Swallow, F.R. Ahmedand, W.H. Barnes, the crystal structure of pascoite, $Ca_3V_{10}O_{28}.17H_2O$, Acta Cryst. C21 (1966) 397-405.

[26] J.M. Nieto, P. Salagre, F. Medina, J.E. Sueiras, Structure of $Sr_3V_{10}O_{28}.22H_2O$, Acta Cryst. C49 (1993) 1879-1883.

[27]A.D. Weeks, E.A. Cisney, A.M. Sherwood, Hummerite and montroseite ,2 vanadium minerals from Montrose contry ,colorado,Am. Mineral. 36 (1951) 326-330.

[28] O.E. Piro, E.L. Varetti, S.A. Brandán, A.B. Altabef., A crystallographic and vibrational study of cesium diaqua bis[tetraaquasodium(I)] decavanadate, $Cs_4[Na_2(H_2O)_{10}](V_{10}O_{28})$, J. Chem. Crystallogr, 33 (2003) 57-63.

[29] M. Graia, R. Ksiksi, A. Driss, Nonapiperidiniummonohydrogen decavanadate tetranitrate, Acta. Cryst. E65 (2009), , m953–m954.

[30] Z.A. Siddiqi, P.K. Sharma, M. Shahid, M. Khalid, Anjuli, A. Siddiqueand, S. Kumar, Superoxide scavenging and antimicrobial activities of novel transition metal complexes of oxydiacetatedianion as primary ligand: Spectral characterization, cyclic voltammetric investigations and crystal structure, Eur. J. Med. Chem. 57 (2012) 102–111.

[31] W.H. Baur, The Geometry of Polyhedral Distortions. Predictive Relationships for the Phosphate Group, Acta Cryst. B30 (1974) 1195-2015.

[32] W.R. Scheldt, Stereochemistry of Low-Spin Cobalt Porphyrins. III. The Crystal Structure and Molecular Stereochemistry of Bis(piperidine)-a,/3,7,5-tetraphenylporphinatocobalt(II) , J. Am. Chem. Soc. 96 (1974) 84–89.

Journal Pre-proof

[33] P. R. Marcoux, B. Hasenknopf, J. Vaissermann, P. Gouzerh, Developing Remote Metal Binding Sites in Heteropolymolybdates, Eur. J. Inorg. Chem, 13 (2003) 2406–2412.

[34] B. Hasenknopf, R. Delmont, P. Herson, P. Gouzerh, Anderson-Type Heteropolymolybdates Containing Tris(alkoxo) Ligands: Synthesis and Structural Characterization, Eur. J. Inorg. Chem. 5 (2002), 1081–1087.

[35] C.M. Liu, Y.H. Huang, D.Q. Zhang, S. Gao, F.C. Jiang, J.Y. Zhang, D.B. Zhu, Bis(ethylenedithio)tetrathiafulvalene Radical Salts with Anderson Type Heteropolymolybdates Containing Tris(alkoxo) Ligands, Cryst. Growth Des. 5 (2005) 1531–1538.

[36]R.L. Frost, K.L. Erickson, M.L. Weierand, O. Carmody, Raman and infrared spectroscopy of selected vanadates, Spectrochim, Acta A 61 (2005) 829–834.

[37] S. Yerra, S. Supriya, S.K. Das, Reversible morphological transition between nano-rods to micro-flowers through micro-hexagonal crystals in a sonochemical synthesis based on a polyoxovanadate compound, Inorg. Chem. Commu. 35 (2013) 54 -57.

[38]K. Nakamoto, Infrared and Raman Spectra of Inorganic and Coordination Compounds, Handbook of Vibrational Spectroscopy, (2006).

[39] M. Cheng, N. Li, N. Wang, K. Hu, Z. Xiao, P. Wu, Y. Wei, Synthesis, structure and antitumor studies of a novel decavanadate complex with a wavelike two-dimensional network, Polyhedron 155(2018) 313-319.

[40] M. Aureliano, Recent perspectives into biochemistry of decavanadate,World J. Biol. Chem. 2 (2011) 215-225.

[41] S.K. Wolff, D.J. Grimwood, J.J. McKinnon, M.J. Turner, D. Jayatilaka, M.A. Spackman, University of Western Australia, 2012.

[42] J.J. McKinnon, D. Jayatilaka, M.A. Spackman, Chem Commun. (2007) 3814 - 3816

[43] M.A. Spackman, J.J. McKinnon, CrystEngComm, 4 (2002) 378-392:

Journal Pre-proof

[44] J.M. Maestre, X. López, C. Bo, J.M. Poblet, N. Casañ-Pastor, Electronic and Magnetic Properties of α-Keggin Anions: A DFT Study of $[XM_{12}O_{40}]^{n-}$, (M = W, Mo; X = Al^{III}, Si^{IV}, P^{V}, Fe^{III}, Co^{II}, Co^{III}) and $[SiM_{11}VO_{40}]^{m-}$ (M = Mo and W),J. Am. Chem. Soc., 123 (2001) 3749–3758.

[45](a) J.A. Fernández, X. Lópe, J.M. Poblet, A DFT study on the effect of metal, anion charge, heteroatom and structure upon the relative basicities of polyoxoanions, J. Mol. Catal. A: Chemical, (2007) 236–242.

(b) P. Kozłowski, A. Notario-Estévez, C. de Graaf, X. López, K. Yu Monakhov, Reconciling the valence state with magnetism in mixed-valentpolyoxometalates: the case of a $\{VO_2F_2@V_{22}O_{54}\}$ cluster, Phys. Chem. Chem. Phys. 19 (2017) 29767–29771.

(c) J.A. Fernández, X. López, C. Bo, C. de Graaf, E.J. Baerends, J.M. Poblet,Polyoxometalates with Internal Cavities: Redox Activity, Basicity, and Cation Encapsulation in $[X^{n+}P_5W_{30}O_{110}]^{(15-n)-}$ Preyssler Complexes, with X=Na^{+}, Ca^{2+}, Y^{3+}, La^{3+}, Ce^{3+}, and Th^{4+}, J. Am. Chem. Soc. 129 (2007) 12244–12253.

[46] J.Y. Kempf, M. M.Rohmer, J.M. Poblet, C. Bo, M. Bénard, Relative Basicities of the Oxygen Sites in $[V_{10}O_{28}]^{6-}$. An Analysis of the ab Initio Determined Distributions of the Electrostatic Potential and of the Laplacian of Charge Density, J. Am. Chem. Soc. 114 (1992) 1136–1146.

Journal Pre-proof

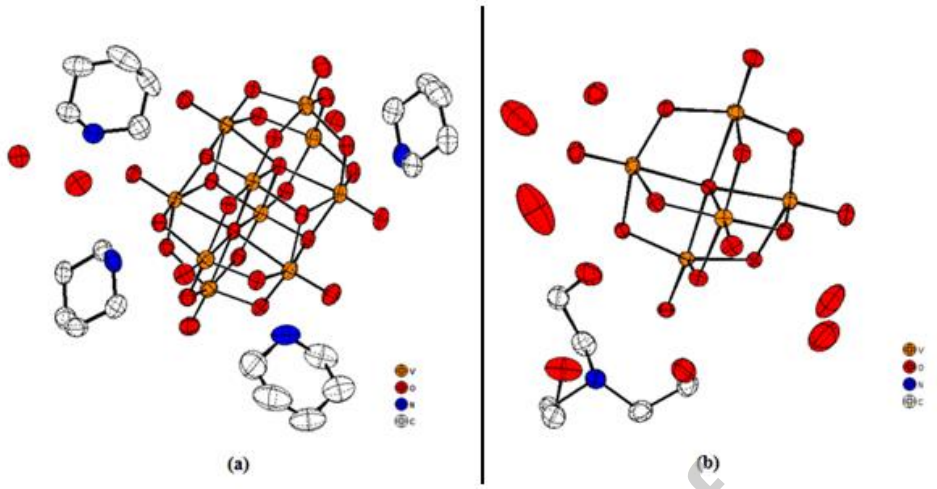

Fig.1.View of the asymmetric unit contents for the crystal structures of compounds (**I**) and (**II**)

Journal Pre-proof

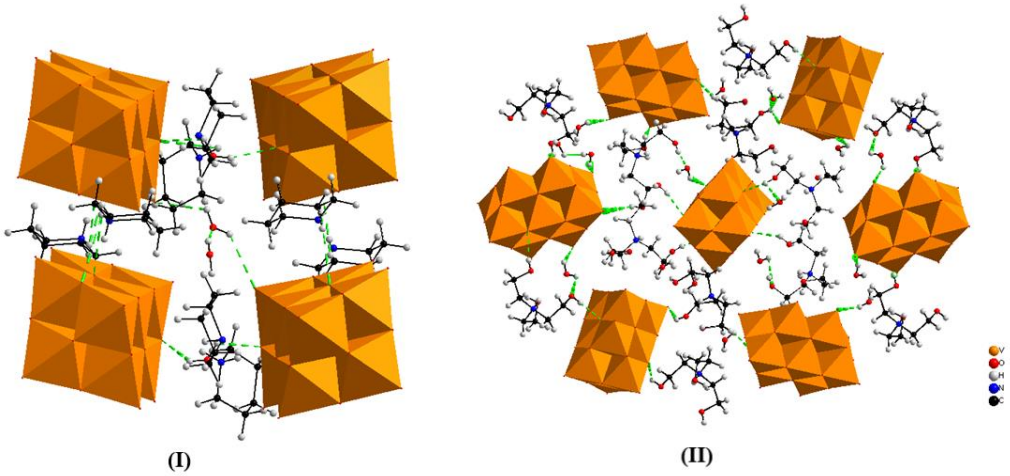

Fig.2. Selected relevant hydrogen bonds structure within the crystal packing of (I) and (II)

Journal Pre-proof

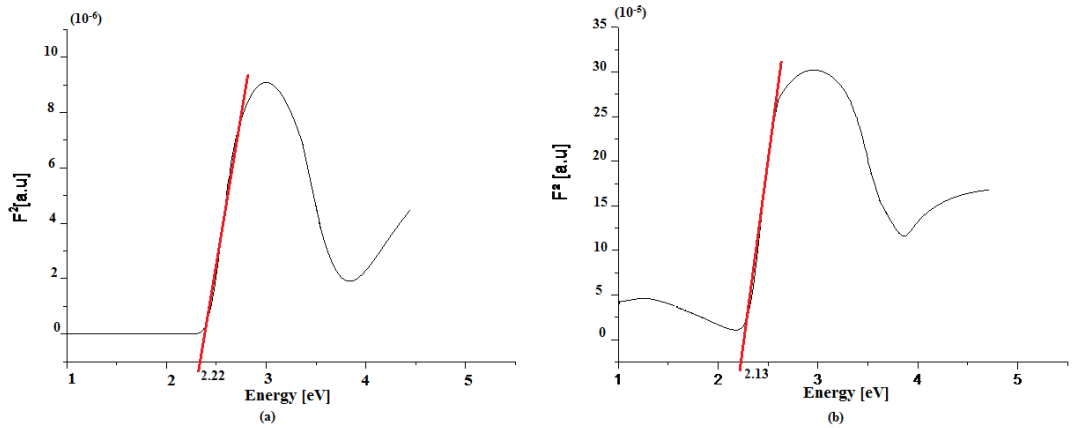

Fig.3. Determination of the optical band gap of compound (**I**) and (**II**) from UV/Vis diffuse reflectance spectrum using the Kubelka-Munk method

Journal Pre-proof

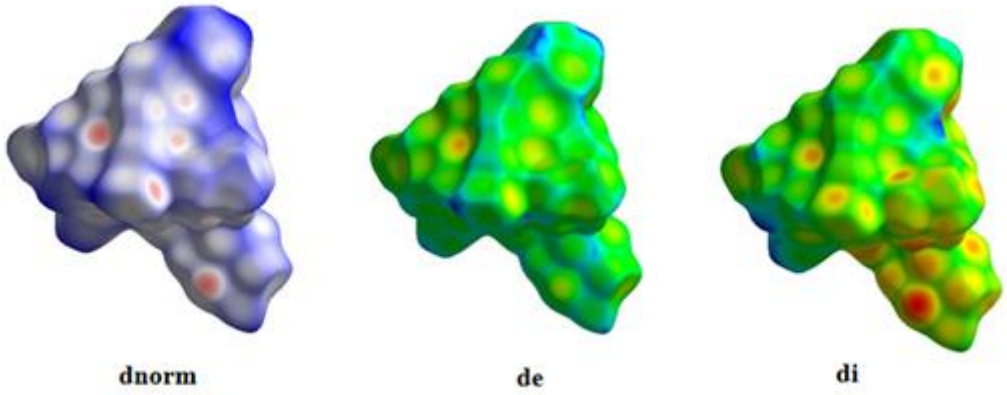

Fig.4. Hirschfield surfaces mapped with d*norm* (mapped over a fixed color scale of -0.656 (red) to 1.884 (blue), de and di of (I)

Journal Pre-proof

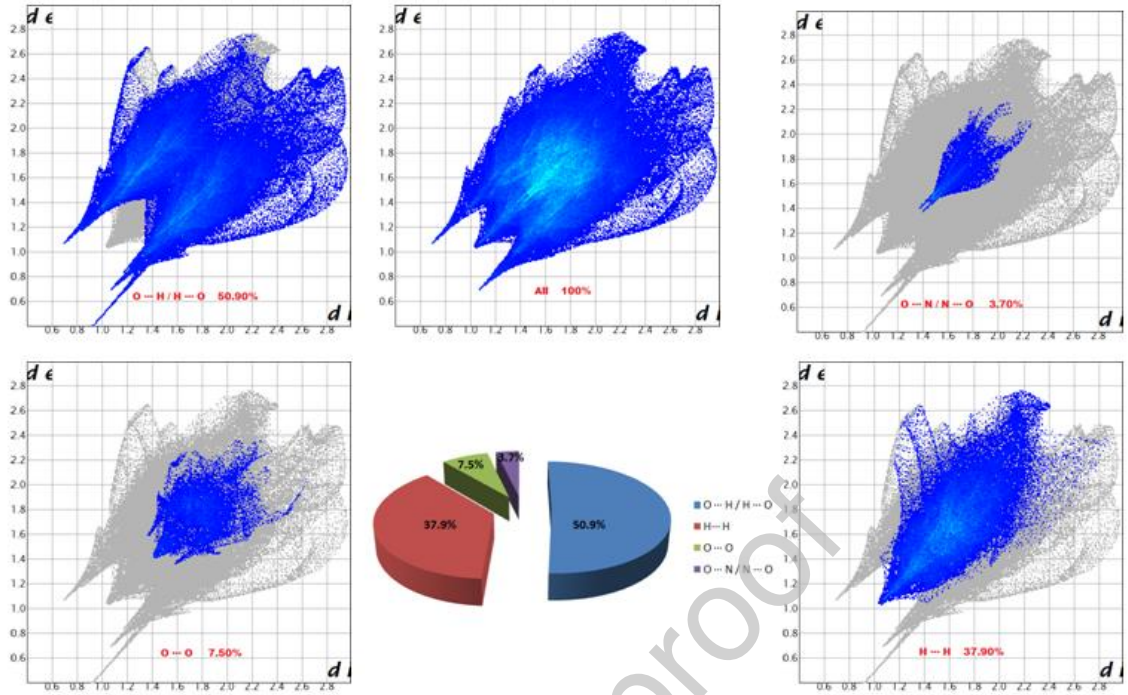

Fig.5. Hirschfield 2D fingerprint plots of **(I)**

Journal Pre-proof

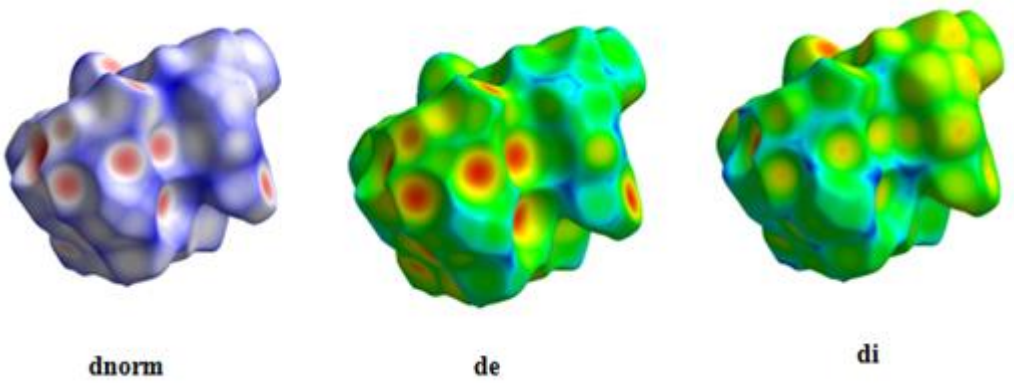

Fig.6. Hirschfield surfaces mapped with dnorm (mapped over a fixed color scale of -1.077 (red) to 1.286 (blue)), de and di of(II)

Journal Pre-proof

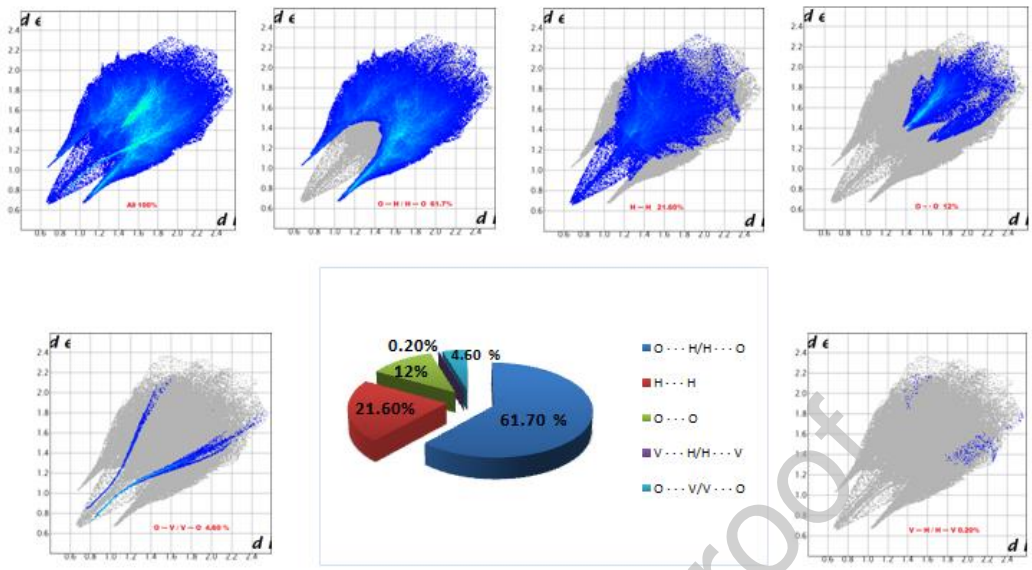

Fig.7. Hirschfield 2D fingerprint plots of (**II**)

Journal Pre-proof

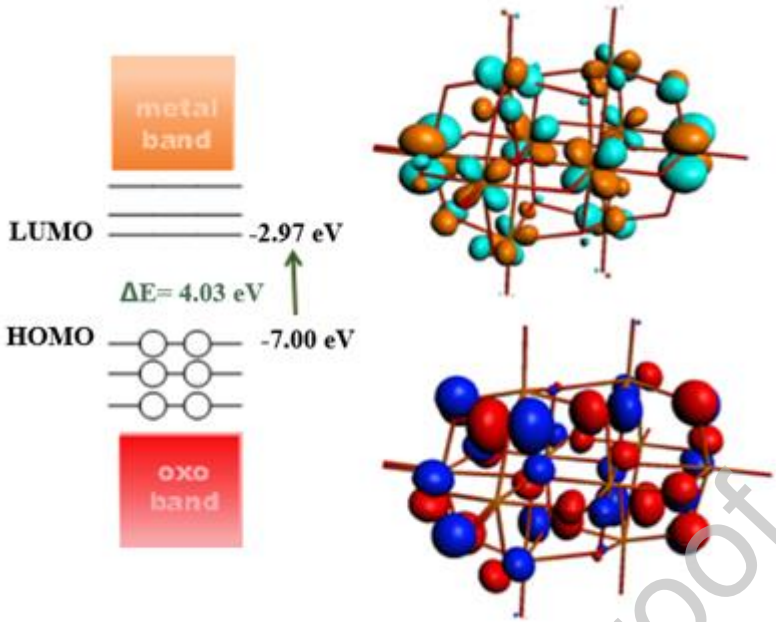

Fig.8. Frontier molecular orbital plots of polyoxoanion $[V_{10}O_{28}]^{6-}$

Journal Pre-proof

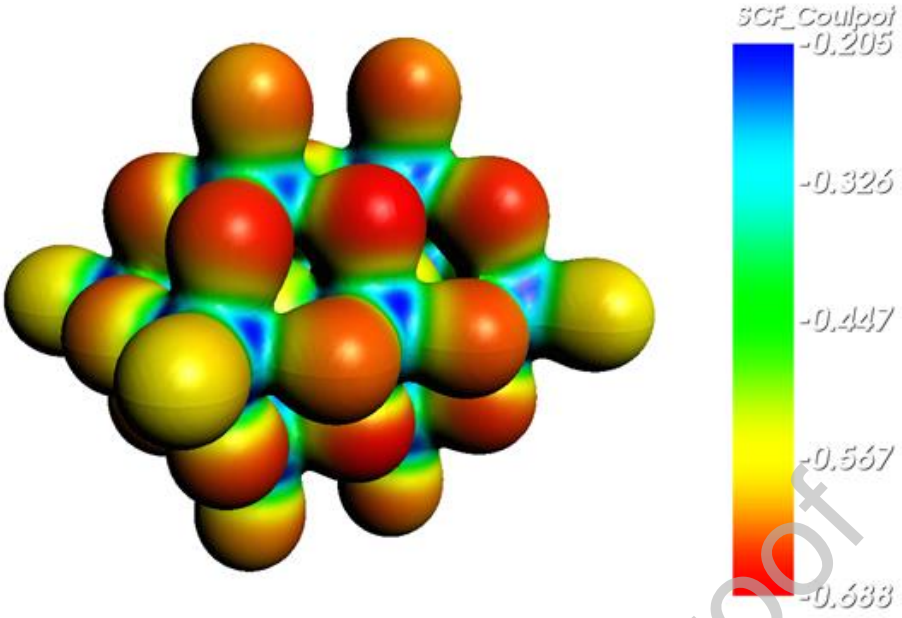

Fig.9. Electrostatic potential (red: more negative potential, blue: less negative potential)

Journal Pre-proof

Table1. Crystal data and structure refinement parameters for Compounds (**I)** and **(II)**

Empirical formula	$(C_5H_{12}N)_4[H_2V_{10}O_{28}]\cdot 3.25H_2O$	$(C_6H_{12}N(OH)_3)\ [H_2V_5O_{14}]\cdot 5H_2O$
Formula weight ($g.mol^{-1}$)	1360.32	717.97
Temperature (K)	293	293
Crystal system	Monoclinic	Orthorhombic
Space group	C2/c	Pbca
a (Å)	28.7460 (5)	16.8955 (3)
b (Å)	19.2130 (5)	13.4818 (2)
c (Å)	18.4853 (4)	19.320 (4)
β (°)	113.374 (1)°	90
V ($Å^3$)	9371.5 (4)	4400.8 (9)
Z_space group	8	8
Crystal density (calc)	1.928	2.167
μ (mm^{-1})	1.99	2.15
F(000)	5458	2872
Index ranges	-37 ≤ h ≤ 37;-25≤ k ≤ 23 ;-22 ≤ l ≤24	-22 ≤ h ≤ 20 ;-17≤ k ≤ 17 ;-25 ≤ l ≤24
Radiation (Å)	Mo Kα(λ = 0.71073)	MoKα (λ = 0.71073)
Reflectionscollected	32950	27787
Independent reflections ;	11134	5221
R_{int}	0.054	0.036
Reflections with I >2σ(I)	6347	4267
Refinedparameters	588	322
S (goodness-of-fit)	0.97	1.06
Final R indexes [I>=2σ(I)]	R_1 = 0.077, wR_2 = 0.130	R_1 = 0.034, wR_2 = 0.102

Journal Pre-proof

$\Delta\rho_{max}/\Delta\rho_{min}$	1.47 eÅ^{-3}/-0.67eÅ^{-3}	0.78 eÅ^{-3}/-0.74 eÅ^{-3}

Table2: Selected bond lengths [Å] for the anion in compound (**I**) (Å)

Bond length (Å)	***X-ray***	***Bond length(Å)***	***X-ray***
V1—O3	*1.696 (3)*	*V6—O2*	*1.825 (3)*
V1—O12	*1.684 (3)*	*V6—O5*	*1.606 (3)*
V1—O13	*1.936 (2)*	*V6—O13*	*2.027 (3)*
V1—O16	*2.173 (3)*	*V6—O14*	*2.012 (3)*
V1—O24	*1.917 (3)*	*V6—O23*	*1.808 (3)*
V1—O27	*2.059 (2)*	*V6—O27*	*2.251 (3)*
V2—O6	*2.064 (3)*	*V7—O12*	*2.088 (3)*
V2—O8	*1.593 (3)*	*V7—O15*	*1.594 (3)*
V2—O18	*1.874 (3)*	*V7—O20*	*1.915 (3)*
V2—O23	*1.876 (3)*	*V7—O26*	*1.837 (3)*
V2—O27	*2.392 (3)*	*V7—O27*	*2.331 (3)*

Journal Pre-proof

Journal Pre-proof

V2—O28	*1.816 (3)*	*V7—O28*	*1.823 (3)*
V3—O4	*1.608 (3)*	*V8—O2*	*1.599 (3)*
V3—O11	*2.010 (3)*	*V8—O18*	*1.795 (3)*
V3—O13	*1.906 (3)*	*V8—O24*	*2.067 (3)*
V3—O14	*2.008 (3)*	*V8—O25*	*1.989 (3)*
V3—O16	*2.243 (3)*	*V8—O26*	*1.849 (3)*
V3—O17	*1.748 (3)*	*V8—O27*	*2.232 (3)*
V4—O3	*2.043 (3)*	*V9—O7*	*1.602 (3)*
V4—O9	*1.598 (3)*	*V9—O16*	*2.272 (3)*
V4—O16	*2.285 (3)*	*V9—O19*	*1.812 (3)*
V4—O17	*1.939 (3)*	*V9—O22*	*1.878 (3)*
V4—O19	*1.851 (3)*	*V9—O24*	*1.956 (3)*
V4—O21	*1.828 (3)*	*V9—O25*	*2.001 (3)*
V5—O1	*1.702 (3)*	*V10—O1*	*2.019 (3)*
V5—O6	*1.680 (3)*	*V10—O10*	*1.601 (3)*
V5—O14	*1.897 (3)*	*V10—O11*	*2.039 (3)*
V5—O16	*2.101 (3)*	*V10—O16*	*2.302 (3)*
V5—O25	*1.936 (3)*	*V10—O21*	*1.822(3)*
V5—O27	*2.126 (3)*	*V10—O22*	*1.808(3)*

Journal Pre-proof

Table 3: Selected bond lengths [Å] for the anion in compound (**II)** (Å)

Bond length (Å)	*X-ray*	*Bond length (Å)*	*X-ray*
V1—O3	1.6085 (16)	V3—O5	1.8833 (16)
V1—O13^{i}	1.8189 (18)	V3—O6	2.0697 (19)
V1—O5	1.8312 (17)	V3—O8	2.2945 (16)
V1—O16	2.0016 (17)	V4—O1	1.6028 (19)
V1—O11	2.0223 (18)	V4—O7^{i}	1.8268 (17)
V1—O8	2.2352 (15)	V4—O4	1.8829 (16)
V2—O6	1.6737 (16)	V4—O13	1.8867 (16)
V2—O9	1.6973 (18)	V4—O9	2.0377 (17)
V2—O11	1.9211 (16)	V4—O8^{i}	2.3263 (17)
V2—O16^{i}	1.9255 (16)	V5—O2	1.6034 (17)
V2—O8	2.0953 (17)	V5—O4	1.8237 (18)
V2—O8^{i}	2.1377 (16)	V5—O12^{i}	1.8393 (17)
V3—O10	1.6046 (18)	V5—O11	2.0017 (16)
V3—O7	1.8279 (18)	V5—O16	2.0108 (17)
V3—O12	1.8809 (17)	V5—O8^{i}	2.2576 (15)

Journal Pre-proof

Table 4: Hydrogen bonds for compound (**I**):

D-H… A	d(D-H)	d(H..A)	<DHA	d(D..A)

O_{W29}-H_{W29A}... O25	0.851	1.977	140.89	2.691
O_{W29}-H_{W29B} ... O20$^{(i)}$	0.851	2.430	118.12	2.929
O_{W30}-H_{W30} ... O31$^{(ii)}$	0.848	2.123	154.77	2.913
O_{W31}-H_{W31A} ...O15$^{(iii)}$	0.851	2.596	115.97	3.066
O_{W31}-H_{W31B} ... O5$^{(iv)}$	0.852	2.401	123.77	2.961
O_{W31}-H_{W31} ... O_{W29}	0.852	2.239	145.88	2.983
N3-H3... O24 $^{(v)}$	0.682	2.094	175.47	2.774
N1-H1 ... O3 $^{(vi)}$	0.749	2.230	157.99	2.938
N1-H1 ... O13 $^{(vii)}$	0.749	2.560	115.77	2.963
N1-H1 ... O17 $^{(viii)}$	0.749	2.552	136.24	3.136
N2-H2 ... O14	0.788	2.568	125.18	3.090
N2-H2 ... O23	0.788	2.115	161.87	2.874
N4-H4 ... O20	0.966	1.822	164.77	2.765

Journal Pre-proof

i:[-x+3/2, y+1/2, -z+3/2]; ii: [x, -y+1, z-1/2]; iii:[-x+3/2, -y+1/2, -z+2]; iv:[-x+3/2, y+1/2, -z+3/2]; v:[-x+3/2, y+1/2, -z+3/2];vi:[-x+3/2, y+1/2, -z+3/2]; vii: [-x+3/2, y+1/2, -z+3/2]; viii: [-x+3/2, y+1/2, -z+3/2]

Table 5: Hydrogen bonds for compound (**II)**:

D-H… A	d(D-H)	d (H..A)	<DHA	d (D..A)
OW22-H22… O17	0.845	1.930	173.62	2.772
OW22-H22… OW20$^{(i)}$	0.877	2.315	115.87	2.811
OW14-H14… O4$^{(ii)}$	0.850	1.949	171.67	2.793
OW14-H14… O13$^{(iii)}$	0.849	2.062	167.21	2.896
O15-H15 … O16$^{(iv)}$	0.820	1.888	167.97	2.696
O17-H17… OW14$^{(v)}$	0.820	1.870	174.02	2.687
O18-H18 … O4$^{(vi)}$	0.820	2.569	137.19	3.219
O18-H18… O9$^{(vii)}$	0.820	2.052	155.09	2.817
OW19-H19… O10$^{(viii)}$	0.851	2.382	154.85	3.172
OW19-H19… O12	0.851	2.569	130.56	3.188
OW19-H19… O11$^{(viiii)}$	0.850	2.026	155.73	2.822
OW20-H20… OW22$^{(x)}$	0.850	2.075	144.45	2.810
OW20-H20… O12	0.849	1.975	158.05	2.781
OW21-H21… O1$^{(xi)}$	0.850	2.170	157.72	2.974
OW21-H21… OW14$^{(xii)}$	0.850	2.625	115.28	3.085
OW21-H21… OW22$^{(xiii)}$	0.849	1.952	164.87	2.780

i:[-x+3/2, y-1/2, z] ;ii : [-x+1, -y+1, -z+1] ;iii : [x, -y+3/2, z-1/2] ;iv :[-x+1, -y+1, -z+1] ; v :[x+1/2, -y+3/2, -z+1] ;vi :[-x+3/2, y+1/2, z] ;vii :[-x+3/2, y+1/2, z] ;

viii :[x-1/2, -y+3/2, -z+1] ;viiii :[x-1/2, -y+3/2, -z+1] ;x :[-x+1, -y+1, -z+1] ;xi : [-x+3/2, y+1/2, z] ;xii : [-x+1, y+1/2, -z+3/2] ; xiii :[-x+1, -y+2, -z+1] ;xiiii :[-x+3/2, y+1/2, z]

Journal Pre-proof

A Graphical abstract

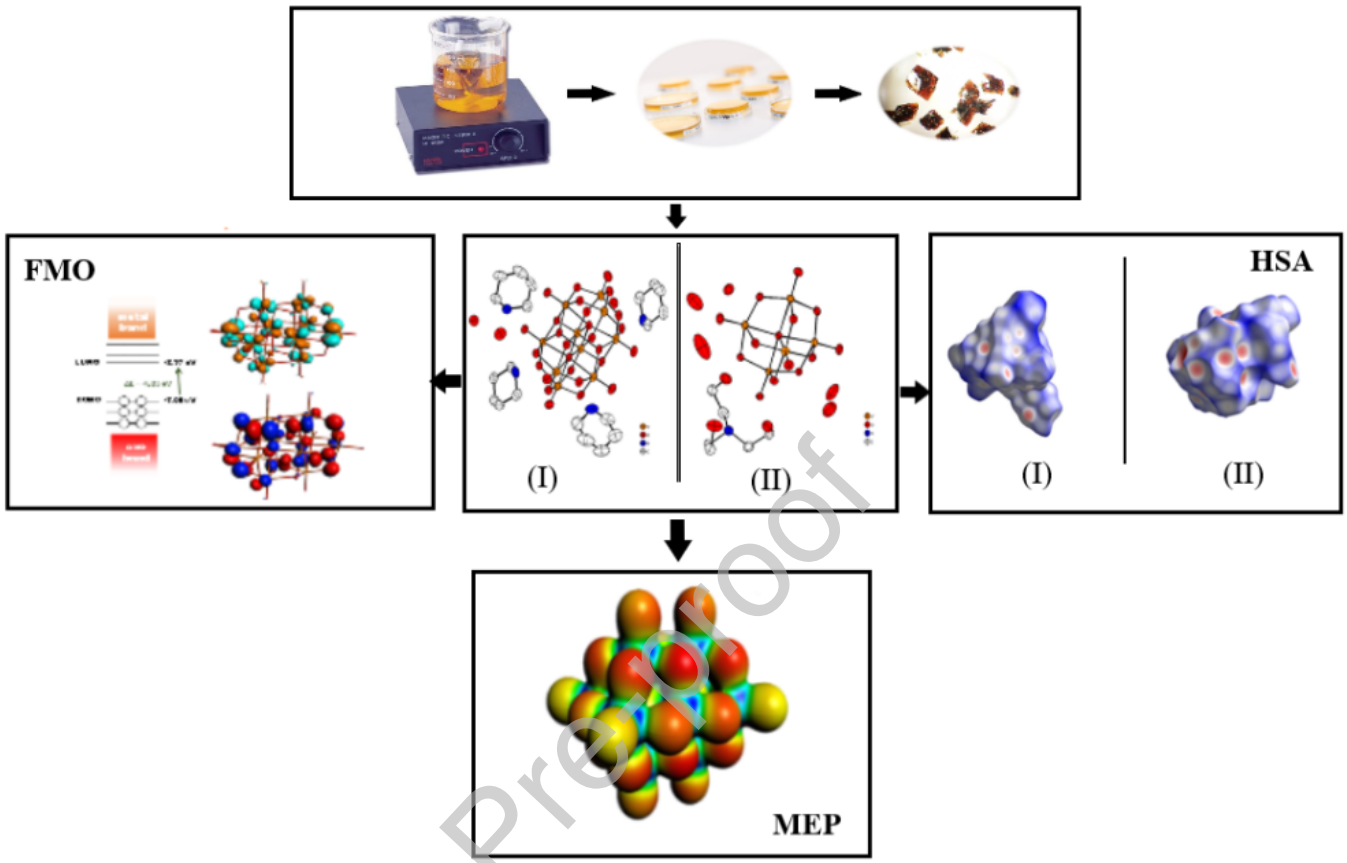

Journal Pre-proof